Articles

Gaseous Complexes of $CoCl_2$ with Pyridine

Claude Daul,* Franzpeter Emmenegger, Michael Mlinar, and Michel Piccand

Institute of Inorganic and Analytical Chemistry, University of Fribourg, Pérolles, CH-1700 Fribourg, Switzerland

Received December 3, 1992

The complex formation of $CoCl_2$ with pyridine in the gas phase has been studied by vapor pressure measurements and by visible spectroscopy at 290–420 °C. A new, very robust fitting procedure has been used to analyze the data. The data analysis not only indicates the presence of two gaseous complexes, $CoCl_2(py)_2(g)$ and $CoCl_2py(g)$, but in addition gives their individual spectra as well as their enthalpy and entropy of formation. The spectra of the two complexes are rationalized by ligand field calculations using published ligand field and Racah parameters.

1. Introduction

When $CoCl_2(py)_2$is heated in a spectrophotometer cell from 290 to 420 °C with a 200- to 1100-fold excess of pyridine, a three-band spectrum (515, 600, 695 nm) develops. The relative absorptions of the bands depend on temperature, pyridine pressure, and py/Co ratio. Figure 1 shows three typical spectra indicating that an increase in temperature and a decrease in excess pyridine have a marked influence on the optical absorption of the gas. To describe our observations of the system, we use three equilibria

$$CoCl_2py(l) \overset{K_1}{\rightleftharpoons} CoCl_2py(g) \qquad (1)$$

$$K_1 = \exp\left(\frac{\Delta S_1}{R} - \frac{\Delta H_1}{RT}\right)$$

$$CoCl_2py(l) + py(g) \overset{K_2}{\rightleftharpoons} CoCl_2(py)_2(g) \qquad (2)$$

$$K_2 = \exp\left(\frac{\Delta S_2}{R} - \frac{\Delta H_2}{RT}\right)$$

$$CoCl_2py(g) + py(g) \overset{K = K_2/K_1}{\rightleftharpoons} CoCl_2(py)_2(g) \qquad (3)$$

plus the mass conservation law if all the Co is evaporated. Finally, the Beer–Lambert law

$$E(\lambda,T) = \epsilon_1(\lambda)\,[CoCl_2py(g)]_T + \epsilon_2(\lambda)\,[CoCl_2(py)_2(g)]_T \qquad (4)$$

relates optical absorbance to concentration.

The data are analyzed using a very robust fitting procedure based on linear programming we recently developed in Fribourg. Using this model, we are able to fit the data of 28 spectra, each one being recorded at a different temperature in seven samples, each of them having a different composition. The fit yields ΔS_i, ΔH_i, and $\epsilon_i(\lambda)$. The final rms deviation is 0.008 absorbance unit.

The observed absorption bands of $CoCl_2py(g)$ and $CoCl_2(py)_2$-(g) are well described using a planar trigonal and a tetrahedral ligand field, respectively.

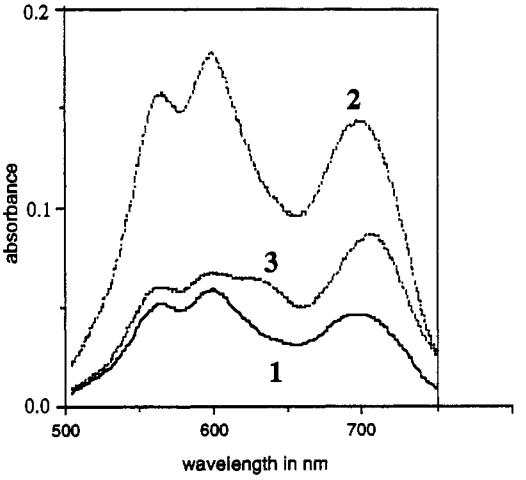

sample No.	Ampoule cm³	[Co] mM	[py] mM	Temp. K
1	29.3	0.0834	52.5	596
2	29.7	0.0770	85	633
3	29.3	0.0851	21	670

Figure 1. Gas-phase spectra of $CoCl_2(py)_n$ ($1 \le n \le 2$).

2. Experimental Section

(a) Chemicals. $CoCl_2py$ and $CoCl_2(py)_2$ were prepared according to ref 1. Pyridine for gas-phase spectroscopy was Merck p.a.

(b) Thermal Analysis. A Mettler TA 3000 system was used for DSC and TG measurements. DSC was used to determine the melting point (200 °C)[4] and the enthalpy of fusion of $CoCl_2(py)_2$. The decomposition reactions I and II (Table I) were investigated by "modified entrainment".[2] In this method the weight loss dW/dt of a sample due to the flow of evolving gases through a precision capillary is converted into vapor pressure. Details of the experimental setup are described in ref 3. Figure

(1) *Gmelin's Handbook of Inorganic Chemistry*, 8th ed.; Verlag Chemie: Weinheim/Bergstrasse, Germany, 1963; Cobalt, Part B, p 62 ff.
(2) Battat, D.; Faktor, M. M.; Garrett, I.; Moss, R. H. *J. Chem. Soc., Faraday Trans. I* **1974**, 2267.
(3) Emmenegger, F. P.; Piccand, M. *Z. Anorg. Allg. Chem.* **1993**, *619*, 17.
(4) Allan, J. R.; Brown, D. H.; Nuttall, R. H.; Sharp, D. W. A. *J. Inorg. Nucl. Chem.* **1964**, *26*, 1895.
(5) Hieber, W.; Woerner, A. *Z. Elektrochem.* **1934**, *40*, 256.
(6) Jacobs, L. J.; van Vuuren, C. P. J. *Transition Met. Chem. (London)* **1989**, *14*, 147.
(7) Lewis, L. C.; Fogel, N. *J. Chem. Soc. A* **1970**, 1141.
(8) Beech, G.; Mortimer, C. T.; Tyler, E. G. *J. Chem. Soc. A* **1967**, 925.

0020-1669/93/1332-2992$04.00/0

Table I. Thermodynamic Cycles[a]

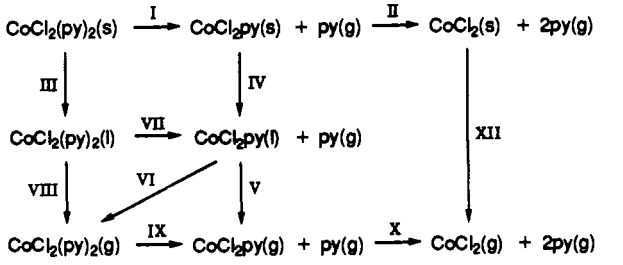

	$\Delta H°$ (kJ mol^{-1})		$\Delta S°$ (J K^{-1} mol^{-1})		
reacn	this work	lit.	this work	lit.	method
I	61.8	64.4–74.0[5,7]	124.1	126.4[7]	mod entrain[3]
II	125.9	101.8[7]	217.5	163.4[7]	mod entrain[3]
I + II	187.7	119.7–189.5[5,7,9]	341.6	290[7]	
III	29.5		62.4		DSC
(IV)	*37.0*				estd
V	163.7		204.1		vis spectrosc
VI	84.0		75.0		vis spectrosc
(VII)	*69.3*				
(VIII)	*153.3*				vis spectrosc
(IX)	*79.7*		*129.1*		
(X)	*159.2*				
(IX + X)	*238.9*	254[10]			
(XII)		234[10]			

[a] Computed and literature values of enthalpies and entropies in the thermodynamic cycle are given in italics, and the reaction number is in parentheses. All of them are related to the standard state of 1 bar.

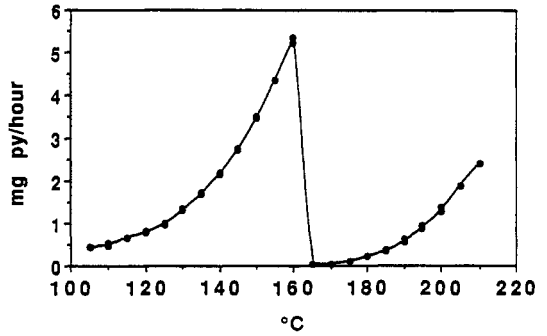

Figure 2. Decomposition of $CoCl_2(py)_2$ (modified entrainment[3]).

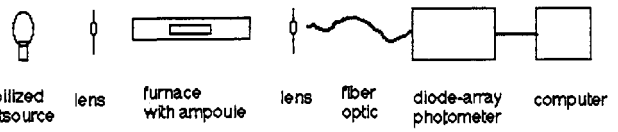

Figure 3. Experimental setup.

2 shows the nicely separated decomposition temperatures of $CoCl_2(py)_2$ and of $CoCl_2py$.

(c) UV–Vis Spectra. Gas-phase spectra were recorded in 10-cm optical quartz cells of a volume of about 29 cm^3. They contained [py] = 21–87 mM and [Co] = 0.077–0.146 mM. The cells were sealed under vacuum and heated in a furnace of 30-cm length. The spectra were recorded by a diode array spectrophotometer (Otsuka, MCPD 1100). The experimental arrangement is schematically represented in Figure 3.

3. Method of Data Analysis

To develop a model that is coherent with the known chemistry of this system and with the observed absorption spectra, we first carry out a principal-component analysis of the data set yielding essentially the number of absorbing species. This initial step is followed by the modeling of the data using a new curve-fitting procedure described in section 3b.

Table II. Principal Component Analysis of Data Set

λ_1	λ_2	λ_3	λ_4
5.9755	0.0509	0.0012	0.0001

(a) Principal-Component Analysis (PCA). The data set obtained from the spectroscopic measurements described in section 2 is represented by a rectangular matrix **M** of absorbances. The columns of this matrix correspond to a particular sample at a given temperature whereas the lines of **M** correspond to a given wavelength. To represent vectors in an n-dimensional space, it is necessary to define the basis of the space and the projections of each data vector on each of the n orthogonal axes. This representation can be expressed in matrix form as

$$\mathbf{M} = \mathbf{C}\mathbf{V}^{\mathrm{T}}$$

where **V** = the matrix containing the orthogonal axes as its columns and **C** = the matrix containing the projection coordinates of each data vector on the basis of the space as its rows. PCA[13] expresses the original data matrix as linear combinations of orthogonal (independent) vectors. These orthogonal vectors define a space that, within experimental errors, contains the same information as the data matrix. To analyze the data vectors according to the principal-component scheme, we use their property to be positive linear combinations of parent, independent vectors. Spectral data that obey the Beer–Lambert law have this property. The columns of **V** are referred to as *eigenvectors*. Associated with each eigenvector is a descriptor of its importance referred to as the *eigenvalue* or singular value λ_i. To account for the variation in the data, the eigenvectors are examined in decreasing order of their eigenvalues. The minimum number of eigenvectors needed to reproduce the data within fixed error limits is taken as the number of independent vectors, n_s. They make up the new data vectors. The PCA of **M** thus yields the number n_s of significant components that, in our case, equals the number of absorbing species. The singular values λ_i of **M** are given in decreasing order in Table II. Only λ_1 and λ_2 are much larger than the experimental uncertainty σ of the absorbance, estimated to be 0.01, and therefore we conclude that two absorbing species are present.

(b) Modeling of the Data. On the basis of this result and some analogy to previously obtained results,[3] a consistent physicochemical model for the complex formation of $CoCl_2$ with py is as given in eqs 1–3, where ΔS_k and ΔH_k are respectively the entropies and enthalpies of formation for steps 1 and 2, R is the universal gas constant, and T is the absolute temperature. We assume that ΔS_k and ΔH_k remain constant within the experimental temperature range. Using this model and remembering that in the actual experiment a large excess of py(g) is used, we can easily obtain the equilibrium concentrations in the gas phase. Two cases have to be considered:

case 1: liquid phase present in the ampule

$$c_{1,i} = [CoCl_2py] = (R'T)^{-1}\exp\left(\frac{\Delta S_1}{R} - \frac{\Delta H_1}{RT_i}\right) \quad (5a)$$

$$c_{2,i} = [CoCl_2(py)_2] = [py]_i \exp\left(\frac{\Delta S_2}{R} - \frac{\Delta H_2}{RT_i}\right) \quad (6a)$$

case 2: *no* liquid phase present in the ampule

$$c_{1,i} = [CoCl_2py] = \frac{c_{\mathrm{tot},i}}{1 + R'T[py]_i \exp\left(\frac{\Delta S_2 - \Delta S_1}{R} - \frac{\Delta H_2 - \Delta H_1}{RT_i}\right)} \quad (5b)$$

$$c_{2,i} = [CoCl_2(py)_2] = \frac{c_{\mathrm{tot},i}}{1 + (R'T)^{-1}[py]_i^{-1} \exp\left(\frac{\Delta S_1 - \Delta S_2}{R} - \frac{\Delta H_1 - \Delta H_2}{RT_i}\right)} \quad (6b)$$

where $[py]_i$ and $c_{\mathrm{tot},i}$ are respectively the concentrations of py(g) and the total gaseous complex; the index i refers to a particular experimental

(9) Beech, G.; Ashcroft, S. J.; Mortimer, C. T. *J. Chem. Soc. A* **1967**, 929.
(10) Burkinshaw, P. M.; Mortimer, C. T. *Coord. Chem. Rev.* **1983**, *48*, 101.
(11) Barin, I.; Knacke, O.; Kubaschewski, O. *Thermochemical properties of inorganic substances (supplement)*; Springer Verlag: Berlin, 1977; pp 174–5.
(12) Kubaschewski, O.; Evans, E. L L.; Alcock, C. B. *Metallurgical Thermochemistry*; Pergamon Press: Oxford, U.K., 1967; pp 370–1.
(13) Sharaf, M. A.; Illman, D. L.; Kowalski, B. R. In *Chemometrics*; Elvings, P. J., Winefordner, J. D.; Kolthoff, I. M., Eds.; Wiley-Interscience: New York, 1989.

condition (column i of matrix M); $R' = 0.08314$ L bar K^{-1} mol^{-1} and $R = 8.314$ J K^{-1} mol^{-1}.

In the Beer–Lambert law, the absorbance E is proportional to concentration. To allow comparison of these results with other studies based on the standard state of 1 bar, the relation $K_p = K_c(R'T)^{\Delta\vartheta}$ ($R' = 0.08314$ L bar K^{-1} mol^{-1}, ϑ = stoichiometric coefficients) has been used in deriving the equations above.

Finally, the Beer–Lambert law yields a prediction of the elements of M as

$$E^{pred}_{j,i} = \epsilon_1(\lambda_j)\, c_{1,i} + \epsilon_2(\lambda_j)\, c_{2,i} \tag{7}$$

where $\epsilon_s(\lambda_j)$ is the absorptivity of species s at wavelength λ_j.

Now, the adjustable parameters ΔS_k, ΔH_k, and $\epsilon_s(\lambda_j)$ can be obtained by minimization of the residuals $r_{j,i}$

$$r_{j,i} = E^{pred}_{j,i} - E^{obs}_{j,i} \tag{8}$$

where $E^{pred}_{j,i}$ and $E^{obs}_{j,i}$ are respectively the predicted (cf. eq 7) and the observed elements of the matrix M. The standard procedure to refine these adjustable parameters is nonlinear least-squares fitting.[14] However, it is our experience that this kind of procedure usually conveys strong correlation among the set of linear parameters, $\epsilon_s(\lambda_j)$, and the set of nonlinear parameters, ΔS_k or ΔH_k. In the present case, only two parameters are nonlinear while the overwhelming number of them are linear. Thus, the application of classical nonlinear least-squares analysis, where all parameters are treated as nonlinear, yields a first subset of absorptivities which are very large and negative and a second one which are very large and positive; the sum of both yields reasonable absorbances. To circumvent this pitfall, we have developed a new procedure, which is presented here. It is based on linear programming.

Step 1: Obtain an initial estimation for ΔS_1, ΔH_1, ΔS_2, and ΔH_2.

Step 2: Compute $c_{s,i}(\Delta S_1, \Delta H_1, \Delta S_2, \Delta H_2)$ using eqs 5 and 6.

Step 3: Compute $\epsilon_s(\lambda_j)$ by linear programming; i.e., consider $r_0 = \max\{|r_{j,i}|\}$, the Chebyshew norm of the residuals. Then, the following inequalities hold:

$$\epsilon_1(\lambda_j)\, c_{1,i} + \epsilon_2(\lambda_j)\, c_{2,i} - E^{obs}_{j,i} \le r_0 \tag{9a}$$

$$-\epsilon_1(\lambda_j)\, c_{1,i} - \epsilon_2(\lambda_j)\, c_{2,i} + E^{obs}_{j,i} \le r_0 \tag{9b}$$

$$\epsilon_1(\lambda_j) \ge 0 \qquad \epsilon_2(\lambda_j) \ge 0 \tag{9c}$$

As $r_0 > 0$, dividing by r_0 yields

$$c_{1,i}x_{1,j} + c_{2,i}x_{2,j} - E^{obs}_{j,i}x_{3,j} \le 1 \tag{10a}$$

$$-c_{1,i}x_{1,j} - c_{2,i}x_{2,j} + E^{obs}_{j,i}x_{3,j} \le 1 \tag{10b}$$

$$x_{s,j} \ge 0 \tag{10c}$$

where $x_{1,j} = \epsilon_1(\lambda_j)/r_0$, $x_{2,j} = \epsilon_2(\lambda_j)/r_0$, and $x_{3,j} = 1/r_0$ subject to the condition

$$-x_{3,j} = \text{minimum} \tag{10d}$$

This system of constraints (10) is nothing but a problem of linear programming,[14] which is easily solved, yielding the linear parameters $\epsilon_s(\lambda_j)$ and the absolute value of the largest residual r_0.

Step 4: Obtain an improved estimation for the nonlinear parameters ΔS_1, ΔH_1, ΔS_2, and ΔH_2 by using the simplex or the conjugate directions search algorithm[14] to minimize $r_0(\Delta S_1, \Delta H_1, \Delta S_2, \Delta H_2)$.

Step 5: If the correction of these latter parameters between two subsequent iterations becomes smaller than the tolerance, stop here; otherwise go to step 2 and repeat steps 2–5 until convergence is achieved.

This procedure is very robust and is now used routinely in our institute. The analysis of our data set (M) with this method yields a good agreement between the observed and predicted absorbances. The largest final deviation r_0 equals 0.02 and the rms deviation is 0.008 absorbance unit.

The equilibrium parameters ΔS_1, ΔH_1, ΔS_2, and ΔH_2 are listed in Table I (K_1 for reaction V, K_2 for reaction VI) while the spectra $\epsilon_s(\lambda_j)$ are presented in Figure 4.

Inspection of Figure 4 shows that the absorption spectrum of $CoCl_2(py)_2$ is characterized by three ligand field bands centered at

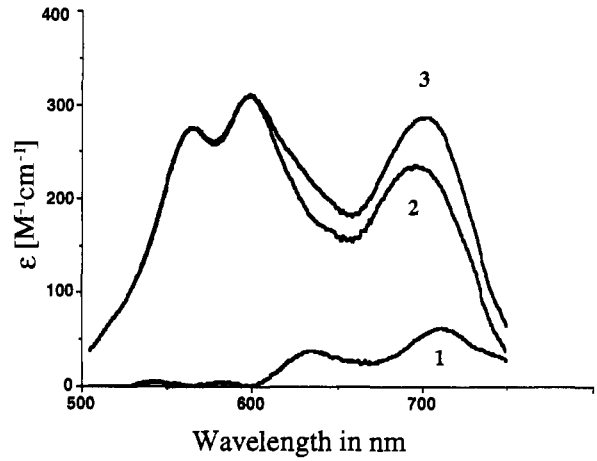

Figure 4. Spectra of $CoCl_2(py)_2(g)$ and $CoCl_2(py)(g)$ and overlay of both: (1) absorptivity of $CoCl_2py$; (2) absorptivity of $CoCl_2(py)_2$; (3) sum of (1) and (2).

$\lambda_{max} = 697$ nm (14 350 cm^{-1}) $\quad \epsilon_{max} = 235$ M^{-1} cm^{-1}

$\lambda_{max} = 599$ nm (16 700 cm^{-1}) $\quad \epsilon_{max} = 310$ M^{-1} cm^{-1}

$\lambda_{max} = 564$ nm (17 730 cm^{-1}) $\quad \epsilon_{max} = 275$ M^{-1} cm^{-1}

whereas the spectrum of $CoCl_2py$ is characterized by two ligand field bands centered at

$\lambda_{max} = 710$ nm (14 080 cm^{-1}) $\quad \epsilon_{max} = 62$ M^{-1} cm^{-1}

$\lambda_{max} = 633$ nm (15 800 cm^{-1}) $\quad \epsilon_{max} = 38$ M^{-1} cm^{-1}

For comparison, the spectra of $CoCl_2(py)_2$ in the gas phase and in toluene are presented in Figure 5. It is noteworthy that the absorption spectra of the uncharged molecular complex $CoCl_2(py)_2$ are remarkably different in the gas phase and in a solvent such as toluene which has very weak donor properties.

4. Structure and Spectra

The absorption spectra of $CoCl_2(py)_2$ and $CoCl_2py$ obtained as a result of the fitting procedure are validated by ligand field calculations.

The ligand field spectrum of tetrahedral $[CoCl_4]^{2-}$ has been already carefully analyzed, and the ligand field parameters of this complex are well-known.[15] We have thus retained Racah's parameter $B = 725$ cm^{-1} for Co and both $e_\sigma = 2500$ cm^{-1} and $e_\pi = 500$ cm^{-1} for Cl corresponding to the best fit of this complex. Next we assumed tetrahedral coordination for $CoCl_2(py)_2$ and trigonal coordination for $CoCl_2py$. Using then this set of approximations, the ligand field state energies given in Table III were obtained by trial and error. Note that the parameters used are similar in all cases.

5. Discussion

Table I gives values in the thermodynamic cycle of the $CoCl_2$/pyridine system. Reactions I and II are reported to occur in two steps each. This is confirmed by our DTG experiments, but in the "modified entrainment" experiments we only observe the overall steps I and II. Our results are closest to the ones reported in ref 7.

Due to decomposition, the melting temperature of $CoCl_2py$ could not be measured, but we estimate the enthalpy of melting of $CoCl_2py$ to be the average of the values for $CoCl_2py$ (29.5 kJ mol^{-1}) and $CoCl_2$ (44.8 kJ mol^{-1}).[11]

(14) Press, W. H.; Flannery, B. P.; Teukolsky, S. A.; Vetterling, W. T. *Numerical Recipes*; Cambridge University Press: Cambridge, U.K., 1986.

(15) Daul, C.; Day, P. *Mol. Phys.* **1977**, *34*, 1707.

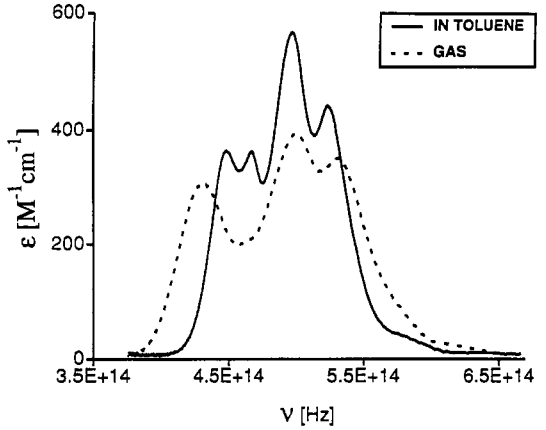

Figure 5. Spectra of $CoCl_2(py)_2$ as a gas and $CoCl_2(py)_2$ dissolved in toluene. The spectrum of the gas has been adjusted to the one in toluene such that both oscillator strengths are the same.

Table III

(a) Energies of the Highest Ligand Field Quartet State of $CoCl_2py$[a]

state	energy (10^3 cm^{-1})	state	energy (10^3 cm^{-1})
$^4A_2(^4F)$	0.000	$^4B_1(^4P)$	13.515
$^4B_2(^4P)$	11.403	$^4A_2(^4P)$	17.004

(b) Ligand Field State Energies of $CoCl_2(py)_2$[b]

state	energy (10^3 cm^{-1})	state	energy (10^3 cm^{-1})
$^4A_2(^4F)$	0.000	$^4A_2(^4P)$	16.234
$^4B_2(^4P)$	14.917	$^4B_1(^4P)$	17.945

[a] Trigonal symmetry and the following set of parameters has been used: $B(Co) = 727$ cm^{-1}, $e_\sigma(Cl) = 2500$ cm^{-1}, $e_\pi(Cl) = 500$ cm^{-1}, $e_\sigma(py) = 5500$ cm^{-1}, $e_\pi(py) = 1100$ cm^{-1}. [b] Tetrahedral symmetry and the following set of parameters has been used: $B(Co) = 727$ cm^{-1}, $e_\sigma(Cl) = 2700$ cm^{-1}, $e_\pi(Cl) = 450$ cm^{-1}, $e_\sigma(py) = 5500$ cm^{-1}, $e_\pi(py) = 1000$ cm^{-1}.

With the estimate for reaction IV, the enthalpy of reaction VII can be estimated. It is reasonable that the enthalpies of reactions I, VII, and IX are not too different because in all cases $CoCl_2(py)_2$ loses one pyridine. This supports our result for reaction IX from the fitting procedure of the optical measurements.

The fitting procedure of the absorbance measurements yields thermodynamic values for reactions V and VI. Values for reactions VI and VII can be used to calculate a value for reaction VIII. This estimate of the enthalpy of reaction VIII shows the similarity of reactions VIII and V, which supports our results for reaction V.

In ref 10 the enthalpy of sublimation of $CoCl_2(py)_2$ is estimated to be 100 kJ mol^{-1} while we find (III + VIII) 182.8 kJ mol^{-1}. For $CoBr_2(py)_2$ an enthalpy of sublimation of 110.5 kJ mol^{-1} is reported.[5]

The enthalpy of sublimation of $CoCl_2$ is rather uncertain. More recent values vary from 218[11] to 258.3 kJ mol^{-1}.[12] Using 234 kJ mol^{-1},[10] the enthalpy of reaction X is 159.2 kJ mol^{-1}. Thus the enthalpy of attaching the first pyridine to $CoCl_2$ is −159.2 kJ mol^{-1}, while that for attachment of the second pyridine is considerably smaller (−79.7 kJ mol^{-1}). The average $CoCl_2$–pyridine bond energy of 119.5 kJ mol^{-1} compares favorably with the value 127 ± 6 kJ mol^{-1} of ref 10 but is lower than the one for $CoBr_2$–pyridine (163.6 kJ mol^{-1}).[3]

According to Christensen et al.,[16] the enthalpy of adding two pyridines to $CoCl_2$ in various organic solvents is −20 to −55 kJ mol^{-1}. This is much less than the value observed for the reaction in the gas phase (−238.9 kJ mol^{-1}), thus indicating that $CoCl_2$ and pyridine have much more negative solvation enthalpies than $CoCl_2(py)_2$.

Ligand Field Spectra. We have demonstrated in section 4 that the ligand field spectra of $[CoCl_4]^{2-}$, $CoCl_2(py)_2$, and $CoCl_2py$ can be described with a ligand field model by using the same Racah and almost the same AOM parameters.

Since the strength of the ligand field is weak, in all three cases the absorption bands in the visible part of the spectrum originate from the parent ^4P state of the free ion. In T_d symmetry ^4P becomes $^4T_1$, whereas in C_{2v} symmetry it is split into $^4A_2$, $^4B_1$, and $^4B_2$.

Though the ligand field model satisfactorily explains the band positions in the visible part of the absorption spectrum, it is surprising that the band intensity is much weaker for trigonal $CoCl_2py$ than it is for tetrahedral $CoCl_2(py)_2$. However, we should point out that the uncertainty attached to the absorptivities of this former complex might be quite important, since over the whole temperature range the fractional part of this species is a few percent only. Thus, the absorbance due to this species is low and the precision of its absorptivity in the fitting procedure is therefore somewhat uncertain. Another likely explanation for this behavior is the following: due to the planar geometry of the molecule, the electric transition moment is only efficient in two spatial directions; i.e., the transition gets intensity from only two of the three components of the electric dipole operator.

Acknowledgment. This work is part of Project 20-29001.90 of the Swiss National Science Foundation.

(16) Christensen, J. J.; Eatough, D. J.; Izatt, R. M. *Handbook of Metal Ligand Heats*, 2nd ed.; Dekker: New York, 1975; p 308.